Magnetic resonance image-guided implantation of chronic recording electrodes in the macaque intraparietal sulcus

H. Scherberger[1], *I. Fineman*[1,2], *S. Musallam*[1], *D. J. Dubowitz*[1,3], *K. A. Bernheim*[1], *B. Pesaran*[1], *B. D. Corneil*[1], *B. Gilliken*[1], *and R. A. Andersen*[1,*]

[1]Division of Biology, California Institute of Technology, Pasadena, CA 91125, USA
[2]Department of Neurosurgery, Huntington Memorial Hospital, Pasadena, CA 91105, USA
[3]Present address: Center for Functional MRI, Department of Radiology, University of California San Diego, La Jolla, CA 92039, USA
*Corresponding author

Keywords: microwire electrodes, magnetic resonance imaging, parietal cortex, neural prosthesis.

Running title: MR image guided chronic electrode implantation

Corresponding address: Richard A. Andersen
Division of Biology, Mail Code 216-76
California Institute of Technology
Pasadena, CA 91125
Tel: (626) 395-8337
Fax: (626) 795-2397
Email: andersen@vis.caltech.edu; hans@vis.caltech.edu

Number of words:	4741
Number of words in abstract:	192
Number of pages:	21
Number of figures:	5

Accepted for publication in the **Journal of Neuroscience Methods**

June 11, 2003

(#NA031303456)

Abstract

The implantation of chronic recording electrodes in the brain has been shown to be a valuable method for simultaneously recording from many neurons. However, precise placement of these electrodes, crucial for successful recording, is challenging if the target area is not on the brain surface. Here we present a stereotaxic implantation procedure to chronically implant bundles of recording electrodes into macaque cortical sulci, employing magnetic resonance (MR) imaging to determine stereotaxic coordinates of target location and sulcus orientation. Using this method in four animals, we recorded simultaneously the spiking activity and the local field potential from the parietal reach region (PRR), located in the medial bank of the intraparietal sulcus, while the animal performed a reach movement task. Fifty percent of all electrodes recorded spiking activity during the first two post-operative months, indicating their placement within cortical gray matter. Chronic neural activity was similar to standard single electrode recordings in PRR, as reported previously. These results indicate that this MR image-guided implantation technique can provide sufficient placement accuracy in cortical sulci and subcortical structures. Moreover, this technique may be useful for future cortical prosthesis applications in humans that require implants within sulci.

Introduction

Recording electrodes have been implanted in the mammalian brain for the purpose of chronic recording of neural activity since the late 1950's (Kruger and Bach, 1981; O'Keefe and Bouma, 1969; for a review see: Schmidt, 1999; Strumwasser, 1958). Chronic multiple single-unit recording has been applied for studying the correlation of neural activity within one or more different brain areas and has provided a new means of recording neural activity under less behaviorally restrained conditions (Fee and Leonardo, 2001; Fryer and Sandler, 1974; Gray et al., 1989; Humphrey et al., 1970). Recent technological progress made it possible to record the spiking activity and the local field potential simultaneously from many tiny electrodes that have been surgically implanted into the brain, while progress in computer technology and digital signal processing allowed analysis of neuronal population signals virtually in real time with a delay of only a few tenths of a second (Donoghue et al., 1998; Isaacs et al., 2000; Kralik et al., 2001). Such rapid decoding of neuronal signals is essential for systems that will control an effector in real time, such as a motor neural prosthesis, which must allow instant interpretation of neural commands in order to effectively interface with a device such as a cursor on a computer screen or a robotic arm (Chapin et al., 1999; Serruya et al., 2002; Taylor et al., 2002; Wessberg et al., 2000).

The majority of research groups working in this field are currently focusing on motor and premotor cortical areas to decode limb movements in real time. In contrast to motor and premotor areas, it has been shown that the motor planning activity in the posterior parietal cortex (PPC) could provide additional, and perhaps superior signals for the online decoding of limb movements (Buneo et al., 2002; Meeker et al., 2002; Pesaran et al.,

2002; Shenoy et al., 2003). For example, the parietal reach region (PRR) in the PPC, seems to represent reach endpoint positions of upcoming limb movements in visual coordinates, rather than the movement trajectory, and plays a prominent role for sensorimotor transformation (Andersen et al., 1998; Scherberger and Andersen, 2003). In contrast to motor cortical areas, the PPC may be less prone to cortical reorganization in patients with spinal cord injuries that suffer from loss of somatosensory feedback (Lotze et al., 1999; Merzenich et al., 1984; Wu and Kaas, 1999), since vision, the dominant sensory input and error correction signal for this area, remains intact.

Surgically, chronic electrode implantation is harder for areas located in the cortical sulcus than for areas on the cortical surface. For chronic recording from PRR, electrode arrays need to be implanted into the medial bank of the intraparietal sulcus (IPS) to a depth of 4-5 mm below the cortical surface (Fig. 1). To target PRR, we have developed a novel microwire electrode implantation technique that employs: magnetic resonance (MR) imaging for stereotaxic electrode placement, electrode arrays specifically designed for PRR, the use of alginate gel to protect the exposed cortex, and a neuro-anesthesia protocol that allows a procedure lengths of 8-10 hours. The improved accuracy of this technique allowed us to place a substantial number of recording electrodes into PRR. In the following, we describe the methods and recording results of four implanted animals.

Methods

All surgical and animal care procedures were in accordance with the National Institute of Health guidelines and were approved by the California Institute of Technology Institutional Animal Care and Use Committee.

To prepare for animal training, a custom-made titanium head post and a dental acrylic head cap (Coralite Duz-All; Bosworth Co., Skokie, Ill) were implanted on each animal in a first surgical procedure. The head cap was secured using titanium bone screws (Synthes, Paoli, PA, USA) for strength in the periphery of the cap and with ceramic screws (Thomas Recording, Germany) around the future skull opening to avoid MR imaging artifacts.

Animal training

Animals were habituated to sit in a primate chair with their heads fixed in front of a back-projected touch-sensitive screen. They were trained to fixate targets on the screen that were illuminated in red and to reach out and touch targets that were illuminated in green, while their eye position was monitored with an infrared video tracking system (Iscan Inc., Cambridge, MA, USA). Using this paradigm, animals performed a delayed center-out reach movement task, in which the animals first touched and fixated a central fixation position and, after a delay period, reached out and touched one of eight peripheral targets at a distance of 20° visual angle. A juice reward was given after each successfully completed trial.

MR imaging

MR imaging was performed using a 1.5 T Siemens Magnetom Vision clinical scanner with a conventional knee coil. A 3D Magnetization Prepared Rapid Acquisition Gradient Echo (MPRAGE) sequence (TR 11.4 ms, TE 4.4 ms, 12 deg flip angle, 250 ms inversion time, 600 ms delay time) with a 128x128 matrix (256x256 with zero-padding) and 141x141 mm field of view was used to acquire 118 sections over a distance of 130 mm

encompassing the entire head of the subject (Dubowitz et al., 2001). Four such runs were signal-averaged and refitted to stereotaxic zero as defined by Reid's plane (intersecting the outer openings of both bony ear canals and the lower rims of both orbits). This rotated composite volume was resliced at 0.5 mm spacing, yielding a final image of voxel size 0.55x0.55x0.5 mm (native resolution: 1.1x1.1x1.0 mm) (Dubowitz, 2002; Pezaris and Dubowitz, 1999). Post-acquisition image analysis was carried out using the AFNI software package (Cox, 1996).

Coronal sections were evaluated, in 2 mm steps from 10 mm posterior to 10 mm anterior of stereotaxic zero, to determine the stereotaxic position and orientation of the IPS. Figure 2 shows an example of a coronal section (at 6 mm posterior) with the right IPS hitting the cortical surface at 9 mm lateral to the medial plane and at an inclination angle of 30°. In each coronal section, a possible electrode position was then determined, such that the entry point at the cortical surface was located 1–2 mm medial to the sulcus to prevent dimpling and the tip of the electrode targeted PRR 4.5 mm below the cortical surface within the medial bank of the IPS (white line).

Electrode arrays

For chronic implantation, electrode arrays were constructed from 75 µm Parelene-C insulated tungsten wire with a sharp tip (diameter: 3 µm) and an impedance of 300 kΩ (MicroProbe Inc., Potomac, MD, USA). 32 such electrodes were arranged in four rows of eight (spacing: 0.4 mm) and attached to two miniature connectors (double row 18-contact, Omnetics Inc., Minneapolis, MN, USA). In addition, one ground and one reference electrode (low impedance) were placed at each end of the array. All electrodes

were rigidly attached to the connector using epoxy glue. Figure 3 shows an electrode array before and during implantation.

Electrode implantation

Anesthesia:

Two days before surgery, the animal was started on anticonvulsants (phenytoin 3 mg/kg daily after 6 mg/kg initially) and oral antibiotics (ampicillin 14 mg/kg and clavulanic acid 2.8 mg/kg).

General anesthesia was induced using ketamine (10 mg/kg IM) and atropine (0.04 mg/kg SC) and maintained using isoflurane (1-2%) after endotrachial intubation. Heart rate, respiratory rate, ECG, non-invasive blood pressure, O_2-saturation, expiratory CO_2, and rectal temperature were continuously monitored throughout the procedure. Venous blood gases were analyzed every 1-2 hours using a tabletop blood gas analyzer (I-STAT, East Windsor, NJ, USA). Fluids were continuously replaced through an IV line at the animal's saphenous vein (lactate Ringer's or saline solution at 50 ml/kg/hour). At the beginning of anesthesia, IM antibiotics (amoxicillin 22 mg/kg), steroids (dexamethasone 1 mg/kg), and analgesics (buprenorphene 0.01 mg/kg IM/ 8 hours) were administered. Additional drugs to control for blood pressure (atropine, dopamine), brain swelling (mannitol, flurosemide), and seizure activity (diazepam, phenytoin) were kept at hand. The animal was mechanically ventilated and moderately hyperventilated (end-tidal CO_2 about 30 mmHg) to reduce brain swelling while the cortical surface was exposed.

Procedure:

The surgical procedure was performed under sterile conditions. After placing the animal in a stereotaxic head holder (David Kopf, Tununga, CA, USA), the existing head cap was removed to expose the skull overlying the parietal cortex. Using a pneumatic drill (Black Max, Anspach Inc., UK), a 2x4 cm hole was made in the skull over the posterior portion of the IPS based on stereotaxic positions from the MR image. The Dura was opened in a 2x5 mm patch determined from the MR images to lie over the most posterior part of medial bank of the IPS, just anterior to the parieto-occipital sulcus, (approximate stereotaxic coordinates: centered on 8 mm posterior, 5 mm lateral). To protect the cortical surface, the dural patch was elevated with a suture before being opened. The stereotaxic positions of the IPS in situ and in the MR images were then compared and in all cases found to be aligned within 2 mm in the axial plane.

To prevent CSF loss, the dural opening was covered with calcium alginate by dropping equal amounts of alginate (Pronova UP LVG: 20mg in 2ml sterile water; Pronova Biomedical, Norway) and calcium chloride solution (1M) on the exposed cortex, which formed a thin layer of protective gel (Becker et al., 2001).

The electrode array was mounted on a stereotaxic arm and positioned above the dura opening. The array was tilted in the coronal plane according to the guidance angle of the corresponding (coronal) MR image (Fig. 2) and rotated about the insertion axis, such that the length of the array was aligned with the IPS along the cortical surface. Figure 3 shows an intra-operative view of the mounted array during insertion. The array was lowered to the cortical surface and then slowly inserted (0.2 mm/min) until the target depth was reached (4-4.5 mm below cortical surface). The cortical surface and the dura

around the electrode were covered with a layer of dural replacement (DuraGen, Integra LifeSciences, Plainsboro, NJ, USA) and a layer of calcium alginate. The inserted array was then fixed to the skull and head cap using dental acrylic before the stereotaxic arm was disconnected from the array. By repeating this procedure, a second electrode array could also be inserted into the medial bank of the IPS. The remainder of the exposed dura was then covered with DuraGen, sealed with calcium alginate against CSF loss, and the skull defect closed with dental acrylic. All arrays were completely embedded in dental acrylic, except for the connector ends. Connectors were protected against dirt and impact by a connector plug and a removable plastic lid that was placed over the arrays and anchored in dental acrylic.

Post-operative care:

After the procedure, the animal was closely monitored for vital and neurological signs. All animals recovered without complications. Systemic analgesics (buprenorphine 0.01 mg/kg SC/8 hours) were administered for several days as needed, to supplement oral analgesia (ibuprophen 5 mg/kg) that was given for 1-2 weeks. Antibiotic medication was administered for two days parenterally (amoxicillin 22 mg/kg IM), then continued orally (ampicillin 14 mg/kg and clavulanic acid 2.8 mg/kg) for 10-14 days. Anticonvulsants were tapered off within the first post-operative week. Animals were allowed to recover completely from surgery (10-14 days) before experiments began.

Recordings

Spiking activity and LFPs were recorded simultaneously from 32-electrodes using a multichannel acquisition processor (MAP, Plexon Inc., Dallas, TX, USA): single units

were isolated online using time-voltage windows and their timing and spike waveforms stored on disk. LFP signals were amplified, low-pass filtered (90 Hz), and digitized as a continuous signal at a sampling rate of 1000 Hz.

Results

Four animals (T, Z, S, C) were implanted with chronic electrode arrays using the surgical technique described above. After full recovery from the procedure, identifiable single-unit spiking activity could be recorded from every implanted electrode array. Overall, 50% of all electrodes (T: 31%, Z: 53%, S: 60%, C: 50%) had identifiable spiking activity during the first two months after implantation, indicating that these electrodes were placed within the gray matter of the IPS. On any given experimental day, clearly identifiable spiking activity was recorded on average from 28% of all electrodes (T: 22%, Z: 25%, S: 35%, C: 32%).

The spatial distribution of electrodes exhibiting spiking activity is given in Fig. 4. Two out of seven arrays (T and Z anterior) showed a strong medio-lateral patterning with many electrodes presenting spiking activity in the two rows adjacent to the IPS while electrodes in the two distant rows had almost no spiking activity. This suggests that these two arrays were only partially inserted into the gray matter of the medial bank of the IPS. In the five other arrays (S, C, and Z posterior), the distribution of electrodes with spiking activity did not show such patterning, suggesting that these arrays were more completely inserted into the target area.

The spiking activity of many units was modulated and showed spatial tuning during a delayed center-out reaching task to 8 peripheral locations (Fig. 5A). Figure 5B shows an example of nine simultaneously recorded single units that were spatially tuned. The

spiking activity of these units show significant, and in some cases even dramatic, differences between reaches to the preferred and the non-preferred target direction, in accordance with previous studies of this area that used the standard single-unit recording technique (Andersen et al., 1997; Kalaska, 1996; Snyder et al., 1997).

In addition to spiking activity, we also recorded the LFP activity from the vast majority of the implanted electrodes (>95 %). The spectral power of the LFP signals was analyzed using multi-taper estimates (Percival and Walden, 1993; Pesaran et al., 2002) and, for many recording sites, showed modulation and directional tuning in the reach movement task, in agreement with a previous report using standard single-unit recording techniques (Scherberger et al., 2001).

Discussion

Using a novel approach to implant multiple electrode arrays with stereotaxic MR imaging guidance, we chronically inserted multiple microwire electrode arrays into the medial bank of the IPS 4-5 mm below the cortical surface with a minimal dural opening. Subsequent simultaneous recordings revealed identifiable spiking activity at about 50% of all implanted electrodes within the first two post-operative months. The pattern of active channels within most of the arrays suggested that the arrays were completely inserted within cortex (the lack of spiking activity on some electrodes being due to their distance from a particular cell rather than being outside of cortex). More generally, our method could be applied to microwire implantation in other brain structures, such as subcortical areas and other cortical sulci (Baker et al., 1999; Deadwyler et al., 1996; Nicolelis et al., 1997).

Key elements for the success of this method are the MR imaging guidance, the design of electrode arrays, particularly sharp electrode tips and an optimized array geometry, as well as the use of alginate gel to protect the exposed cortex against damage and to minimize brain shift associated with loss of cerebro-spinal fluid. In addition, a neuro-anesthesia protocol similar to human neurosurgical practice allowed us to safely extend the procedure to 8-10 hours. During the procedures the animals were intubated and blood gases, fluid balances, and electrolytes were carefully monitored and controlled (Kralik et al., 2001; Logothetis et al., 1999).

Verification of electrode placement with histology was not part of this study, since all animals are currently alive and part of ongoing studies. We are nonetheless convinced that the majority of electrodes are implanted in the proper target location (PRR) for the following reasons: First, Dubowitz (2002) showed that the use of MR image-guided stereotaxic coordinates has an accuracy of 1.3±0.3 mm. Second, our technique involves the direct visualization of the IPS during surgery, which further improves the placement accuracy. Finally and most importantly, our recordings confirm physiologically that the electrodes are in the target area: spiking activity identifies 50% of all electrodes to lie in gray matter and many of those signals show significant directional tuning for reaching. Furthermore, we tested the neural activity in two animals (C, S) using both delayed saccade and delayed reach tasks and found the neural responses significantly larger for reach movements than for saccades, as expected for PRR (Snyder et al., 1998). While we are therefore confident that our electrodes are accurately placed in PRR, we nevertheless plan to develop a positive placement verification method, like post-surgical MR imaging, which will become important in particular for implantations in less explored brain areas.

Neural Prosthesis

The ability to accurately place a substantial number of electrodes into a specified cortical area is particularly important in the emerging field of neural prosthetics, where large populations of neurons need to be decoded online to predict the trajectory or end-position of impending limb movements. Several groups have chronically implanted electrode arrays in motor areas predominantly on the cortical surface and were able to use the simultaneously recorded single- and multi-unit activity to control a robotic or a virtual arm: Nicolelis and colleagues implanted blunt microwires both in the rat and in new-world (owl) monkeys (Chapin et al., 1999; Kralik et al., 2001; Nicolelis et al., 1999; Wessberg et al., 2000), while Schwartz and colleagues implanted microwire arrays with sharp tips into the cortical surface of old-world monkeys (macaques) (Isaacs et al., 2000; Taylor et al., 2002). Similar results were also found by Donoghue and colleagues using micro-machined silicon 100-electrode arrays (Bionics Inc, Utah, USA) that were pneumatically inserted into the macaque premotor and motor areas (Hatsopoulos et al., 1998; Serruya et al., 2002).

Our approach allows us to record reach-movement related spiking activity and the LFP simultaneously from many electrodes in PRR of old world monkeys, which is located within a cortical sulcus. This method could be advantageous in general for electrode implantation in primates with a high degree of encephalization, where a substantial amount of cortex is localized in cortical sulci, and for human implants, where the encephalization is even greater. We have used the signals from the array implants to successfully decode online the intended reach trajectories without the animals emitting any behavior. These results will be reported in a subsequent publication.

Acknowledgement

We thank K. Weaver for animal care, R. Bhattacharyya, B. Greger and V. Shcherbatyuk for technical support, and A. Schwartz, and J. Williams for early, helpful discussions. This work was supported by the Christopher Reeve Paralysis Foundation (HS), the Human Frontier Science Program (BDC), the James G. Boswell Foundation, the Defense Advanced Research Projects Agency, and the National Eye Institute.

Figure legends

Figure 1

Lateral view and coronal section of a macaque brain. A: Lateral view. Gray mark: cortical surface area above the parietal reach region (PRR). B: Coronal section of one cortical hemisphere (6 mm posterior of inter-aural line; marked by dotted line in A). Gray area: PRR, located in the medial bank of the intraparietal sulcus (IPS).

Figure 2

Magnetic resonance image, coronal section (6 mm posterior of inter-aural line). White line: intended electrode array insertion with the tip of the electrodes located in the medial bank of the intraparietal sulcus (IPS), about 4.5 mm below the cortical surface. L: left side. Scale: 1 cm. Fine dark lines: stereotaxic coordinate frame axes.

Figure 3

Intra-surgical view of microwire electrode insertion. Surgical layers from center to periphery: cortex (C), dura (D), skull bone (B), and dental acrylic head cap (H). Horizontal arrow: posterior direction at midline, downward arrow: rightward direction. Curved thick line: right intraparietal sulcus (IPS). Electrode array (A) is connected to a stereotaxic holding apparatus (ST) with its electrode tips penetrating the medial bank of the IPS. Inset: Microwire array (MicroProbe Inc.) with 32 recording electrodes.

Figure 4

Spatial distribution of electrodes with spiking activity. Implanted PRR electrode arrays (one in animal T, two each in animals Z, S, and C) are presented as array schematics (8x4

circles) that are positioned according to the array location within PRR (posterior or anterior) and the IPS (black line). Filled circles: electrodes that presented spiking activity at least for one day during the first two post-operative months. Open circles: electrodes with no spiking activity.

Figure 5

Spiking activity during the delayed reaching task. (A) Time axis of the delayed center-out reach movement task. After the animal fixated and touched a central fixation point (not shown), a visual cue was presented in 1 out of 8 possible target locations for 0.3 sec (gray horizontal bar). In a variable delay period (1.2–1.5 sec), the animal then had to plan, but not execute, a reach movement to that target, until the central fixation point was extinguished, which served as a Go-signal (arrowhead) for the start of the movement (square: mean time when target was acquired). Target directions were randomly interleaved in subsequent trials. (B) Example of 9 simultaneously recorded spiking units (#1–9) that show spatial tuning during this task. Spiking activity is presented in the preferred and non-preferred direction of each unit. In each panel, spike rasters (with individual rows of dots depicting the timing of action potentials during one trial) are presented on top of a peristimulus time histogram that illustrates the trial-averaged spiking activity (at least 40 trials). Spike rasters and histograms are aligned to the cue offset (0 sec). All units show significant tuning in the cue, delay, or movement period.

References

Andersen RA, Snyder LH, Batista AP, Buneo CA, Cohen YE. Posterior parietal areas specialized for eye movements (LIP) and reach (PRR) using a common coordinate frame. In: Bock GR and Goode JA, editors. Novartis Foundation Symposium 218: Sensory Guidance of Movement. Chichester: Wiley, 1998: 109-128.

Andersen RA, Snyder LH, Bradley DC, Xing J. Multimodal representation of space in the posterior parietal cortex and its use in planning movements. Annu Rev Neurosci 1997; 20: 303-30.

Baker SN, Philbin N, Spinks R, Pinches EM, Wolpert DM, MacManus DG, et al. Multiple single unit recording in the cortex of monkeys using independently moveable microelectrodes. J Neurosci Methods 1999; 94: 5-17.

Becker TA, Kipke DR, Brandon T. Calcium alginate gel: a biocompatible and mechanically stable polymer for endovascular embolization. J Biomed Mater Res 2001; 54: 76-86.

Buneo CA, Jarvis MR, Batista AP, Andersen RA. Direct visuomotor transformations for reaching. Nature 2002; 416: 632-636.

Chapin JK, Moxon KA, Markowitz RS, Nicolelis ML. Real-time control of a robot arm using simultaneously recorded neurons in the motor cortex. Nature Neuroscience 1999; 2: 664-670.

Cox RW. AFNI: Software for analysis and visualization of functional magnetic resonance neuroimages. Computers and Biomedical Research 1996; 29: 162-173.

Deadwyler SA, Bunn T, Hampson RE. Hippocampal ensemble activity during spatial delayed-nonmatch-to-sample performance in rats. J Neurosci 1996; 16: 354-72.

Donoghue JP, Sanes JN, Hatsopoulos NG, Gaal G. Neural discharge and local field potential oscillations in primate motor cortex during voluntary movements. J Neurophysiol 1998; 79: 159-73.

Dubowitz DJ. Functional Magnetic Resonance Imaging in Rhesus Macaque Monkeys. Ph.D. thesis in Computation and Neural Systems. Pasadena: California Institute of Technology, 2002.

Dubowitz DJ, Chen DY, Atkinson DJ, Scadeng M, Martinez A, Andersen MB, et al. Direct comparison of visual cortex activation in human and non-human primates using functional magnetic resonance imaging. J Neurosci Methods 2001; 107: 71-80.

Fee MS, Leonardo A. Miniature motorized microdrive and commutator system for chronic neural recording in small animals. J Neurosci Methods 2001; 112: 83-94.

Fryer TB, Sandler H. A review of implant telemetry systems. Biotelemetry 1974; 1: 351-374.

Gray CM, Konig P, Engel AK, Singer W. Oscillatory responses in cat visual cortex exhibit inter-columnar synchronization which reflects global stimulus properties. Nature 1989; 338: 334-7.

Hatsopoulos NG, Ojakangas CL, Paninski L, Donoghue JP. Information about movement direction obtained from synchronous activity of motor cortical neurons. Proc Natl Acad Sci U S A 1998; 95: 15706-11.

Humphrey DR, Schmidt EM, Thompson WD. Predicting measures of motor performance from multiple cortical spike trains. Science 1970; 170: 758-62.

Isaacs RE, Weber DJ, Schwartz AB. Work toward real-time control of a cortical neural prothesis. IEEE Trans Rehabil Eng 2000; 8: 196-8.

Kalaska JF. Parietal cortex area 5 and visuomotor behavior. Can J Physiol Pharmacol 1996; 74: 483-98.

Kralik JD, Dimitrov DF, Krupa DJ, Katz DB, Cohen D, Nicolelis MA. Techniques for long-term multisite neuronal ensemble recordings in behaving animals. Methods 2001; 25: 121-50.

Kruger J, Bach M. Simultaneous recording with 30 microelectrodes in monkey visual cortex. Exp Brain Res 1981; 41: 191-4.

Logothetis NK, Guggenberger H, Peled S, Pauls J. Functional imaging of the monkey brain. Nat Neurosci 1999; 2: 555-62.

Lotze M, Laubis-Herrmann U, Topka H, Grodd W. Reorganization in the primary motor cortex after spinal cord injury - a functional magnetic resonance (fMRI) study. Restorative Neurology and Neuroscience 1999; 14: 183-187.

Meeker D, Cao S, Burdick JW, Andersen RA. Rapid plasticity in the parietal reach region demonstrated with a brain - computer interface. Society of Neuroscience Abstracts 2002; 28: 357.7.

Merzenich MM, Nelson RJ, Stryker MP, Cynader MS, Schoppmann A, Zook JM. Somatosensory cortical map changes following digit amputation in adult monkeys. J Comp Neurol 1984; 224: 591-605.

Nicolelis MA, Ghazanfar AA, Faggin BM, Votaw S, Oliveira LM. Reconstructing the engram: simultaneous, multisite, many single neuron recordings. Neuron 1997; 18: 529-37.

Nicolelis MAL, Stambaugh CR, Brisben A, Laubach M. Methods for simultaneous multisite ensemble recordings in behaving primates. In: Nicolelis MAL, editor. Methods for Neural Ensemble Recordings. Boca Raton, London, New York: CRC Press, 1999: 121-156.

O'Keefe J, Bouma H. Complex sensory properties of certain amygdala units in the freely moving cat. Experimental Neurology 1969; 23: 384.

Percival DB, Walden AT. Spectral analysis for physical applications - multitaper and conventional univariate techniques. Cambridge, MA: Cambridge University Press, 1993.

Pesaran B, Pezaris JS, Sahani M, Mitra PP, Andersen RA. Temporal structure in neuronal activity during working memory in macaque parietal cortex. Nat Neurosci 2002; 5: 805-11.

Pezaris JS, Dubowitz DJ. MRI Localization of Extracellular Electrodes Using Metallic Deposition at 1.5T. Proc of Int Soc Magn Res Med. Vol 2, 1999: 968.

Scherberger H, Andersen RA. Senosorimotor transformations. In: Chalupa LM and Werner JS, editors. The Visual Neurosciences. Vol (in press). Cambridge, MA: MIT Press, 2003: 1324-1336.

Scherberger H, Jarvis M, Andersen RA. Properties of the local field potential in the macaque posterior parietal cortex during arm-reaching movements. 11th annual

meeting of the Society for the Neural Control of Movement. (http://www-ncm.cs.umass.edu), 2001.

Schmidt EM. Electrodes for many single neuron recordings. In: Nicolelis MAL, editor. Methods for Neural Ensemble Recordings. Boca Raton, London, New York: CRC Press, 1999: 1-23.

Serruya MD, Hatsopoulos NG, Paninski L, Fellows MR, Donoghue JP. Brain-machine interface: Instant neural control of a movement signal. Nature 2002; 416: 141-2.

Shenoy KV, Meeker D, Cao S, Kureshi SA, Pesaran B, Buneo CA, et al. Neural prosthetic control signals from plan activity. Neuroreport 2003; 14: 591-6.

Snyder LH, Batista AP, Andersen RA. Coding of intention in the posterior parietal cortex. Nature 1997; 386: 167-70.

Snyder LH, Batista AP, Andersen RA. Change in motor plan, without a change in the spatial locus of attention, modulates activity in posterior parietal cortex. J Neurophysiol 1998; 79: 2814-9.

Strumwasser F. Long-term recording from single neurons in brain of unrestrained mammals. Science 1958; 127: 469.

Taylor DM, Tillery SI, Schwartz AB. Direct cortical control of 3D neuroprosthetic devices. Science 2002; 296: 1829-32.

Wessberg J, Stambaugh CR, Kralik JD, Beck PD, Laubach M, Chapin JK, et al. Real-time prediction of hand trajectory by ensembles of cortical neurons in primates. Nature 2000; 408: 361-365.

Wu CW-H, Kaas JH. Reorganization in primary motor cortex of primates with long-standing therapeutic amputations. Journal of Neuroscience 1999; 19: 7679-7697.

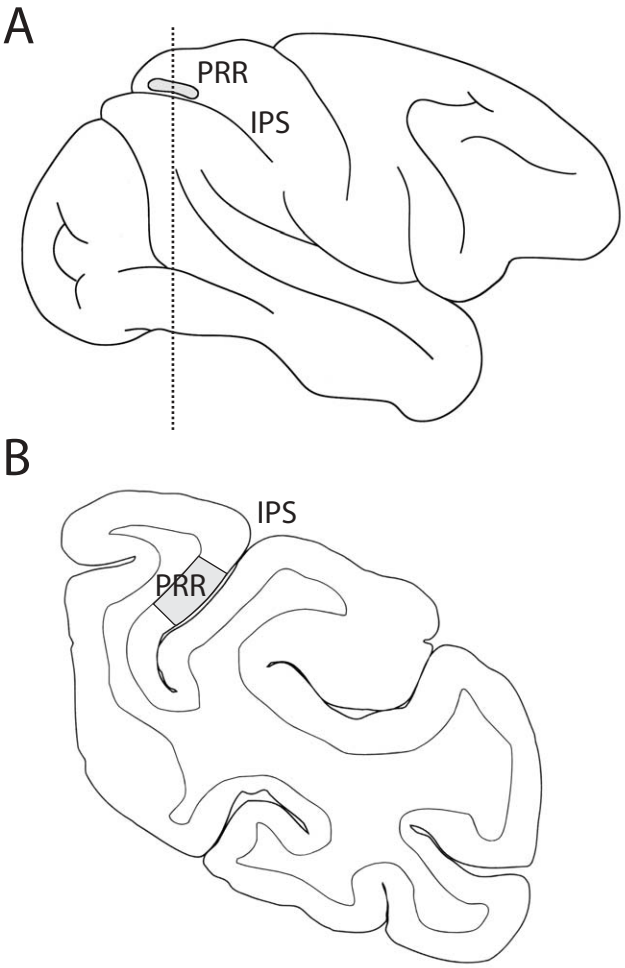

Scherberger, Fig 1

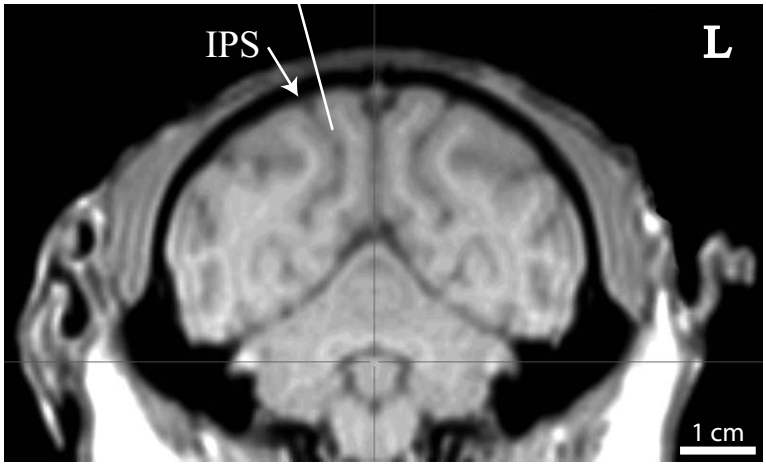

Scherberger, Fig. 2

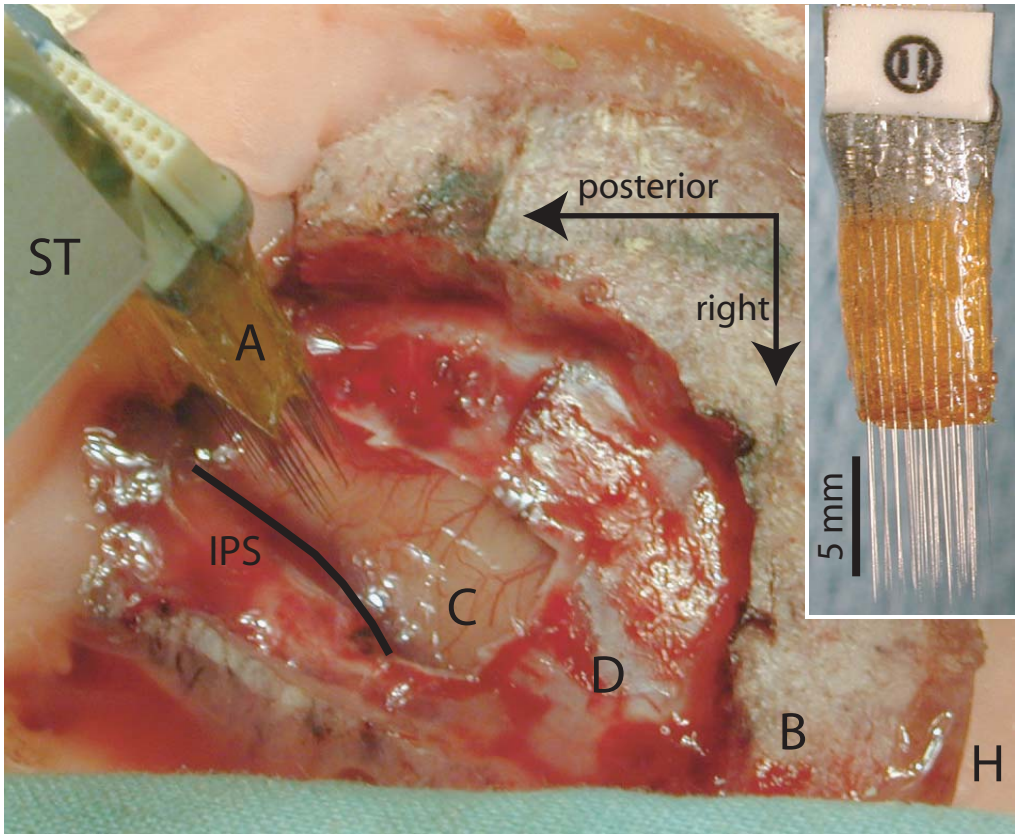

Scherberger, Fig 3

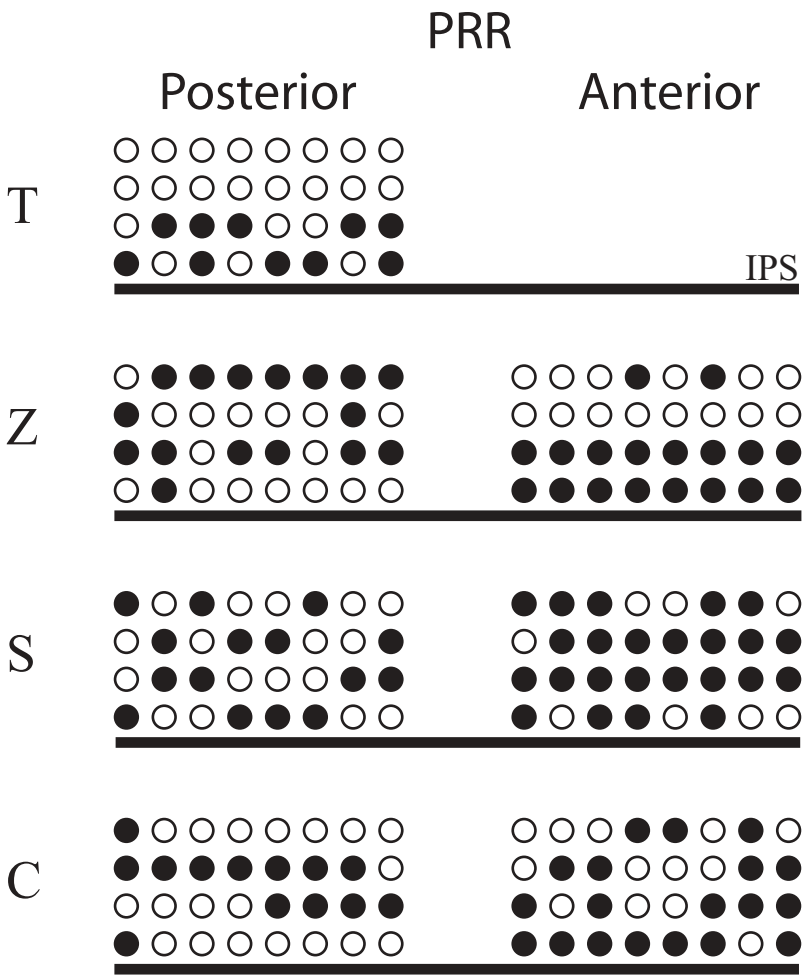

Scherberger, Fig 4

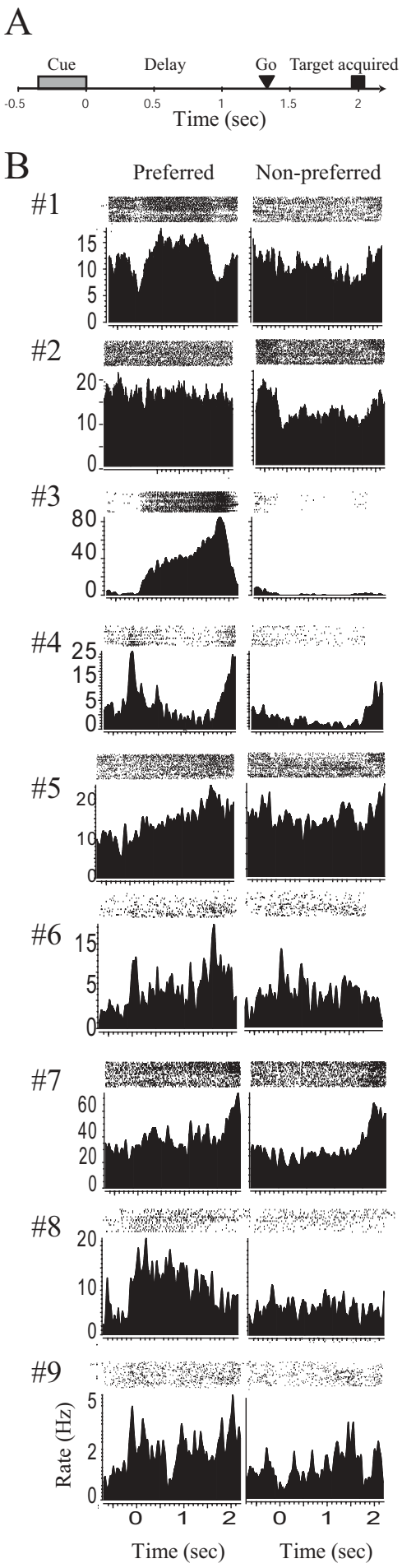

Scherberger, Fig 5